J Nanostruct 11(1): 181-188, Winter 2021

RESEARCH PAPER

Synthesis of NiO Nanoparticles and Sulfur, and Nitrogen co Doped-Graphene Quantum Dots/ NiO Nanocomposites for Antibacterial Application

Sarmad Ghazi Al-Shawi[1,*], Natalia Andreevna Alekhina[2], Surendar Aravindhan[3], Lakshmi Thangavelu[3], Akulina Elena[4], Natalia Viktorovna Kartamyshev[5], and Rafina Rafkatovna Zakieva[6]

[1] *Food Science Department-Agriculture College-Basrah University, Basrah 00964, Iraq*

[2] *Department of regulatory affairs in the sphere of drugs products and medical devices, Medical University of the Ministry of Health of the Russian Federation*

[3] *Department of Pharmacology, saveetha dental College and hospital, saveetha institute of medical and technical sciences,chennai, india*

[4] *Department of Humanities and Socio-Economic Disciplines Associate Professor, K G Razumovsky Moscow State University of technologies and management, Moscow, Russian Federation*

[5] *Department of theory and history of state and law, Southwest State University, Kursk, Russian Federation*

[6] *Department of Industrial electronics and lighting engineering, Kazan State Power Engineering University, Russian Federation*

ARTICLE INFO

Article History:
Received 19 August 2020
Accepted 14 December 2020
Published 01 January 2021

Keywords:
Antibacterial
Disk diffusion
Graphene quantum dots
Nanoparticles

ABSTRACT

The human life is faced with bacterial infections which are one of the major cause of prevalence and mortality. Antibiotics have long been the preferred therapy for bacterial infections due to their cost-effectiveness and efficacy. In the field of overcoming microbial issues, new and emerging nanostructure-based materials have gotten a lot of attention. In this Study, NiO and sulfur, and nitrogen co doped-graphene quantum dots-decorated NiO nanocomposites (S,N-GQDs/NiO) are prepared via a simple hydrothermal method. Structural and morphological properties of products are determined via XRD, SEM, UV-Vis, and FTIR analysis. The prepared products are applied for the investigation of antibacterial activity against P*seudomonas aeruginosa, Escherichia coli, Staphylococcus aureus, and methicillin resistant Staphylococcus aureus (MRSA)*. The results showed that prepared S,N-GQDs/NiO nanocomposites have high antibacterial activity against *Staphylococcus aureus* among a wide range of microorganisms. For S,N-GQDs/NiO nanocomposites nanoparticles, the disk diffusion test proved that the highest growth inhibition zone was related to *Staphylococcus aureus* (17 mm). The presence of graphene quantum dots in S,N-GQDs/NiO nanocomposites facilitates reactive oxygen species (ROS) mechanism which lead to bet antibacterial activity.

How to cite this article
Ghazi Al-Shawi S., Andreevna Alekhina N., Aravindhan S., Thangavelu L., Elena A, Viktorovna Kartamyshev N, Rafkatovna Zakieva R. Synthesis of NiO Nanoparticles and Sulfur, and Nitrogen co Doped-Graphene Quantum Dots/ NiO Nanocomposites for Antibacterial Application. J Nanostruct, 2021; 11(1): 181-188. DOI: 10.22052/JNS.2021.01.019

INTRODUCTION

Bacterial infections, which is one of the great human problems it has faced, causes 16 million death annually in the world [1-3]. So far, many efforts have been done for solving this issue, for example, the use of antibiotics, which become

* *Corresponding Author Email: sarmadghazi@yahoo.com*

very common in 21st century. But the problem is that by taking too many antibiotics, resistance to these antibiotics is has been created [4-6]. So, resistance is a major issue in overcoming the bacterial infections. This requires the provision of new solutions that can be affordable and no destructive environmental and health effects. In recent years, with the advent of nanoscience and nanotechnology, various nanomaterials for the use of antibacterial application have been used [7-10]. Nanomaterials have been considered by various researchers due to their unique physical and chemical characteristics. One of the attractive features of nanomaterials is that their properties are intensively dependent on size and morphology [11-13]. Therefore, the desired properties can be achieved by controlling the shape and their size. Metal oxide nanoparticles have found many applications in different fields in recent years [14, 15]. Nickel oxide nanoparticles, as a metal oxide nanoparticle, have attractive properties such as chemical stability, thermal stability, biocompatibility, and interesting optical properties. To improve the properties of nanomaterials based on nickel oxide, various methods have been adopted. These methods include doping, composite formation with other nanomaterials, as well as control and size control. The purpose of the formation of nanocomposite is to improve the properties of nickel oxide nanoparticles for better antibacterial activity [16-20].

In recent years, graphene quantum dots (GQDs) have attracted much attention as a new member of carbon nanostructures. GQDs have been identified as new kinds of quantum dots with sizes less than 10 nm. GQDs are zero-dimensional (0D) nanostructures with carbon atoms arranged in an sp^2 hybridization pattern. It should be noted that the great advantage of GQDs is the environmentally friendly, which makes it an attractive option in different applications due to its non-toxic properties [21, 22].

K. Karthik et al. prepared CdO–NiO–ZnO mixed metal oxide nanocomposite via a simple microwave method. They investigated the structural properties of products via SEM, XRD, and EDS analysis. They measured nanosheet size 139 nm via TEM analysis. Antibacterial activity of CdO–NiO–ZnO nanocomposite at different concentrations was performed in-vitro against gram negative i.e. E*scherichia coli, Pseudomonas aeruginosa, proteus mirablis, Aeromonas hydrophila, Salmonella typhi and Vibrio cholerae;* gram positive bacteria (G + Ve): *Staphylococcus aureus, Rhodococcus rhodochrous and Bacillus subtilis*. Confocal laser scanning microscopy confirms the rupture of the bacterial cell wall [23].

In another work, nickel oxide-copper oxide-reduced graphene oxide (NiO-CuO-RGO) with different amounts of GO, was synthesized via Gonamanda Satya Sree et al. The prepared products were characterized via XRD, FTIR, Raman spectroscopy, and FESEM analysis. They applied prepared nanocomposites for the investigation of photocatalytic and antibacterial activity. The results showed that NiO-CuO-10%RGO can degrade 91% Brilliant green after 60 min under visible light irradiation. Also, the prepared NiO-CuO-10%RGO nanocomposites show high antibacterial activity against tested microorganisms [24].

The preparation and application of NiO-based nanomaterials have been faced with substantial issues. In the present work, green and simple methods were applied for the preparation of NiO/GQDs nanocomposites. The structural and morphological properties of products were characterized via FESEM, XRD, FTIR, and EDS analysis. Then, the inhibitory and bactericidal properties of synthesized samples were studied toward various Gram-positive and Gram-negative bacteria comprehensively.

MATERIALS AND METHODS

Apparatus and chemicals

The crystallinity and crystal phases of the prepared samples were characterized by X-ray diffraction (XRD; Philips-X'pertpro) Ni-filtered Cu Kα radiation. The functional group of prepared products were analyzed via recording Fourier transform infrared (FT-IR):Nicolet Magna-550 spectrometer in KBr pellets. The size and shape of as-prepared samples were investigated via scanning electron microscopy (SEM:LEO-1455VP equipped with an energy dispersive X-ray spectroscopy). The entire chemicals used in this investigation were of analytical grade: $Ni(COOCH_3)_2.4H_2O$ (99.5%), ammonium hydroxide, citric acid (99.5%), thiourea (TU)(99%), from Merck.

Synthesis of S,N- GQDs

S,N-GQDs was synthesized based on the previously reported paper [25]. Briefly, 0.42g of citric acid was dissolved in 30 ml deionized water and 0.45g thiourea was dissolved in 40 ml

deionized water separately. The thiourea-based solution was added to the solution of citric acid under vigorous stirring. The prepared transparent solution was transferred into Teflon-lined stainless autoclave and heated to 160 °C for 5 hours. The prepared solution was centrifuged under 12000 rpm for 10 min. The prepared S,N-GQDs was stored at 4 ˚C for further experiments.

Synthesis of NiO NPs

The 0.6g $Ni(COOCH_3)_2.4H_2O$ was dissolved in 30 ml deionized water under stirring. The ammonium hydroxide solution was added to the $Ni(COOCH_3)_2.4H_2O$ solution drop by drop. After 60 min, the obtained suspension was transferred to into Teflon lined stainless autoclave and heated to 130 °C for 12 hours. The prepared dark solid was centrifuged and collected. The solid was washed with ethanol and water several times and dried at 50 ˚C for 30 h.

Synthesis of NiO/S,N-GQDs Nanocomposites

The 0.6g $Ni(COOCH_3)_2.4H_2O$ was dissolved in 20 ml as-prepared S,N-GQDs solution under stirring and ambient conditions. In another container, the ammonium hydroxide was dissolved in deionized water to raise pH to 11. The ammonium hydroxide solution was added to Ni-containing solution drop-wise. After 60 min, the as-obtained suspension was transferred into Teflon-lined stainless autoclave and heated to 130 °C for 12 hours. The obtained black solid was centrifuged under 6000 rpm for 10 min and dried at 50 ˚C for 30 h.

Determination of the minimum inhibitory concentration (MIC)

The minimum inhibitory concentration of nanomaterials was measured through the broth microdilution method according to the Clinical and Laboratory Standards Institute (CLSI) guidelines. Mueller Hinton Mueller-Hinton agar plates of NiO and NiO/S,N-GQDs were added to each well. The tests were used 0.5 McFarland standard bacterial suspension of *Pseudomonas aeruginosa, Escherichia coli, Staphylococcus aureus, and methicillin resistant Staphylococcus aureus (MRSA)*. The plates were incubated at 37 ˚C for 18–20 hours. The lowest concentration of NiO and NiO/S,N-GQDs that inhibited the growth of bacteria was provided as minimum inhibitory concentration (MIC).

Determination of the Minimum Bactericidal Concentration (MBC)

The minimum bactericidal concentration (MBC) was determined via the CLSI guidelines (Wayne, 2004). After performing of the MIC test, 10 μL from each clear well-containing nanomaterials was subcultured to Mueller Hinton agar (Becton Dickinson, USA). The plates were incubated in ambient air for 24 hours at 37°C. Visually, the colony-forming units (CFU) were calculated. The MBC was described as the concentration at which bacterial growth was reduced by three logs (>99.9%) when compared to the initial inoculum.

Agar disk-diffusion method

Commercial blank discs impregnated with NiO and NiO/S,N-GQDs were mounted on Muller Hinton agar plates and incubated for 20 hours at 37 ˚C. The clear zone of inhibition was then measured to the nearest millimeter to assess antibacterial activity.

Time-kill curve

A time-kill curve was developed to investigate the rate and degree of bacterial reduction when treated with a NiO and NiO/S,N-GQDs. The inoculums of bacteria were modified to 10^6 CFU/mL. The NiO and NiO/S,N-GQDs were tested against MRSA at 0.25 MIC, 0.5MIC, 1MIC, and 2MIC. At 0, 6, 12, 18, and 24 hours, samples were collected and aliquoted onto BHI agar plates. After a 24-hour incubation period at 37°C, the number of colonies on the BHI plates was measured in CFU/mL.

RESULTS AND DISCUSSION

XRD analysis was applied for the investigation crystalline structure of prepared nanomaterials. As well as shown in Fig. 1a, NiO nanoparticles was formed in rhombohedra phase (JCPDS: 22-1189) with space group of R-3m and cell constants a = 2.9540 Å, b = 2.9540 Å, and c = 7.2360 Å. XRD analysis confirmed the formation of NiO nanoparticles with any impurity. Scherrer equation was utilized to determine crystalline,

$Dc = K\lambda/\beta Cos\theta$

where β is the width of the observed diffraction peak at its half maximum intensity (FWHM), K is the shape factor, which takes a value of about 0.9, and λ is the X-ray wavelength (CuKα radiation, equals to 0.154 nm). The crystalline size was calculated 41 nm for NiO nanoparticles. The XRD pattern of prepared S,N-GQDs was presented in

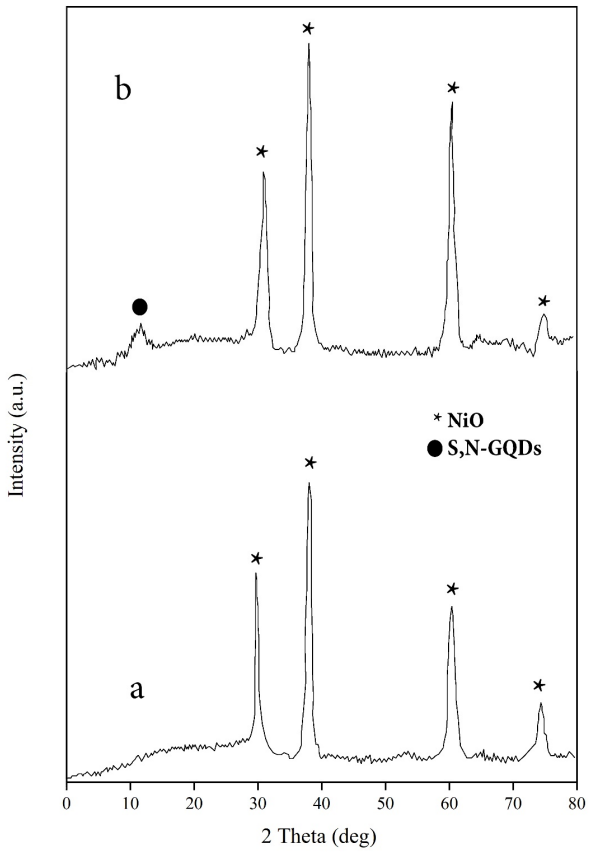

Fig. 1. XRD pattern of as-prepared a) NiO nanoparticles and b) S,N-GQDs/NiO nanocomposites

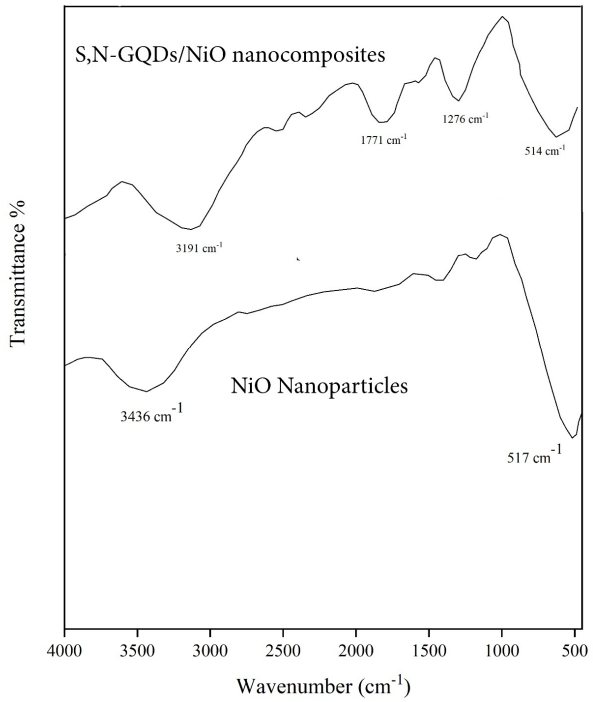

Fig. 2. FTIR spectrum of synthesized NiO nanoparticles and S,N-GQDs/NiO nanocomposites

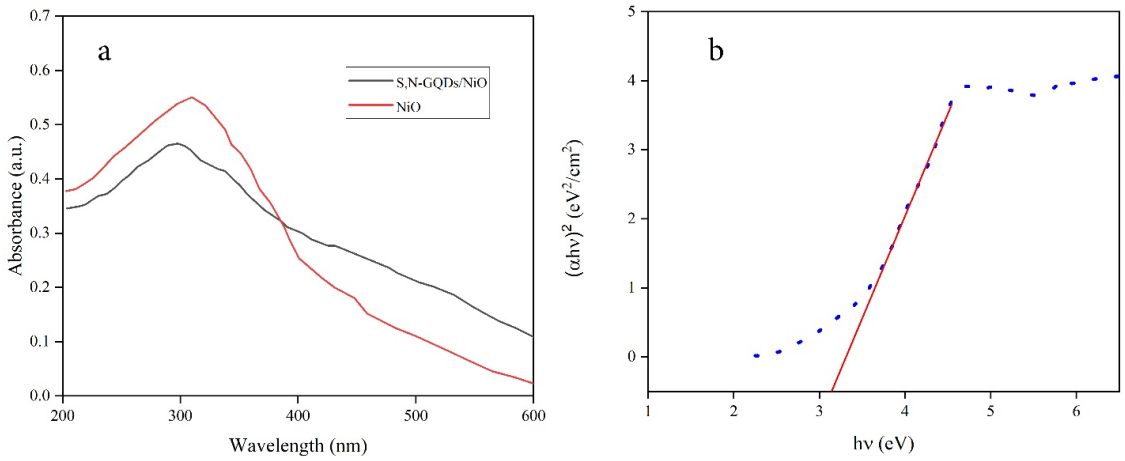

Fig. 3. a) UV-Vis spectrum of NiO nanoparticles and S,N-GQDs/NiO nanocomposites b) band gap (E_g) of NiO nanoparticles

Fig. 2b. The broad peak at 24˚ relates to GQDs. XRD pattern of prepared S,N-GQDs is in good agreement with previously reported work [26]. Fig.1c shows the XRD pattern of prepared S,N-GQDs/NiO nanocomposites. XRD pattern reveals the formation of NiO nanoparticles and S,N-GQDs together. In comparison with XRD pattern of NiO nanoparticles, it is found that the width of peaks has been slightly changed in S,N-GQDs/NiO nanocomposites.

FTIR analysis was applied for investigation functional group of samples. Since the surface of GQDs contains different functional groups, so FTIR analysis can be helpful for the analysis of products. As well as shown, the broad peak at 3000 to 3550 cm^{-1} related to the stretching vibration of the hydrogen bonded OH groups of the adsorbed water, and the peak at 480 cm^{-1} is attributed to Ni-O stretching mode. In the S,N-GQDs/NiO nanocomposites some peaks are observed in 1000-1400 cm^{-1} which is attributed to GQDs-related functional group. The FTIR analysis confirms the linking of S,N-GQDs into NiO nanoparticles clearly.

FESEM analysis was applied for morphological investigation of products. Fig. 3a, and Fig. 3b presents SEM images of as-prepared NiO nanoparticles at two different magnifications. It can be concluded that homogenous 75nm NiO nanoparticles are synthesized via the applied procedure. Fig. 3c, and Fig. 3d shows SEM images of S,N-GQDs/NiO nanocomposites at two magnifications. The images confirm the formation of very tiny GQDs alongside NiO nanoparticles. It is found that the size of NiO nanoparticles in pure NiO and S,N-GQDs/NiO nanocomposites are different significantly. It can be attributed to the applied synthesis procedure of S,N-GQDs/NiO nanocomposites which use S,N-GQDs solution instead of water. The S,N-GQDs and water provide different pH that can be lead to different sizes. Also S,N-GQDs act as a capping agent and prevent the agglomeration of NiO nanoparticles.

The optical properties of NiO nanoparticles and S,N-GQDs/NiO nanocomposites were studied via UV-Vis analysis. Fig. 4 displays UV-Vis spectrum of prepared NiO nanoparticles and S,N-GQDs/NiO nanocomposites. As well as shown in Fig. 4a, the optical absorption was centered at 314 nm for NiO nanoparticles. Fig. 4a shows UV-Vis absorption of S,N-GQDs/NiO nanocomposites. As well as known, the band gap of S,N-GQDs is lower than NiO nanoparticles. This leads to absorption and excitement of S,N-GQDs/NiO via visible light. It can be concluded that absorption extends to the visible region via S,N-GQDs in the S,N-GQDs/NiO nanocomposites.

The optical direct band gap of NiO nanoparticles was measured 3.16 eV via Tauc's relation (Fig. 4b):

$$(\alpha h\upsilon)^2 = \alpha_0(h\upsilon - E_g)$$

Where hυ, α_0 and E_g are photon energy, a constant, and optical band gap respectively.

The results of the broth microdilution procedure were used to determine the MIC and MBC, as shown in Table 1. As well as concluded from Table 1, *Staphylococcus aureus* shows the highest sensitivity since the lowest concentration

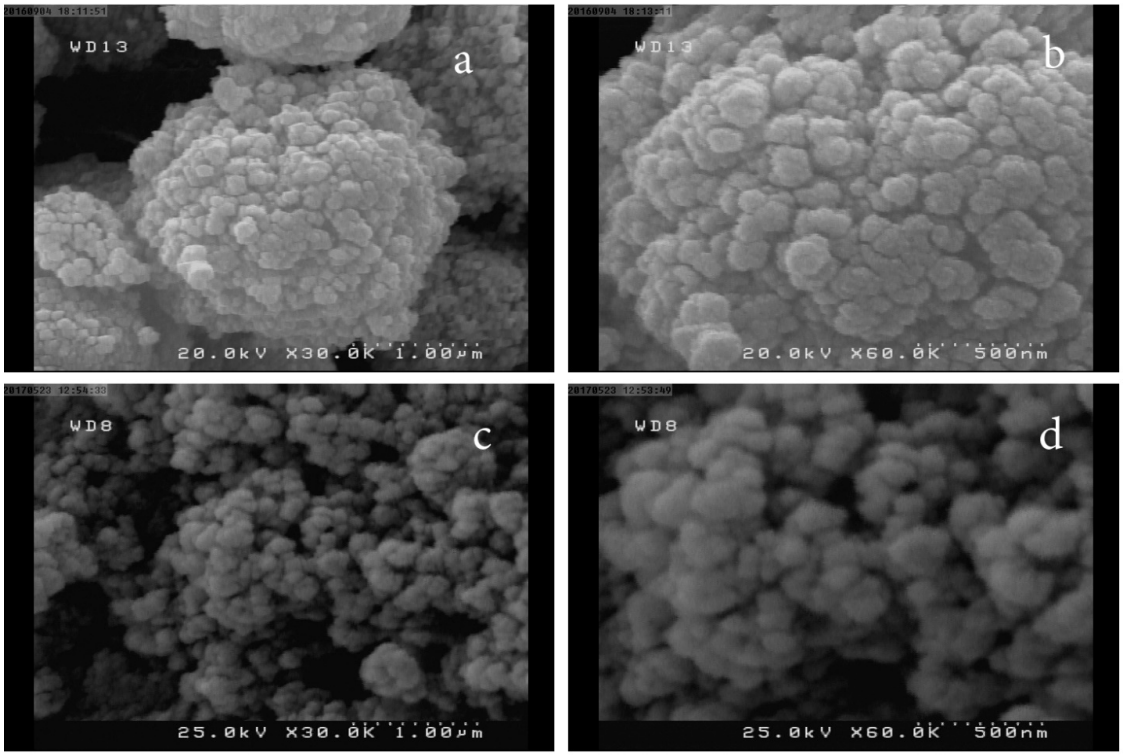

Fig. 4. SEM images of prepared a,b) NiO nanoparticles, b) S,N-GQDs/NiO nanocomposites

Table 1. MIC and MBC value of NiO nanoparticles and S,N-GQDs/NiO nanocomposites against microorganisms

Microorganism	NiO nanoparticles		NiO/S,N-GQDs	
	MIC(mg/ml)	MBC(mg/ml)	MIC(mg/ml)	MBC(mg/ml)
Staphylococcus aureus	0.4	0.8	0.2	0.4
MRSA	0.8	1.6	0.4	0.8
Pseudomonas aeruginosa	0.4	1.6	0.2	1.6
Escherichia coli	0.8	1.6	0.8	1.6

Table 2. Zone of inhibition provided NiO nanoparticles and S,N-GQDs/NiO nanocomposites

Microrganism	Inhibition zones (mm)	
	NiO	S,N-GQDs/NiO
Staphylococcus aureus	16	19
MRSA	11	14
Pseudomonas aeruginosa	8	10
Escherichia coli	10	16

of S,N-GQDs/NiO nanocomposites was applied via MIC and MBC value 0.2 and 0.4 mg/ml. It is clear that inhibition and bactericidal effect of S,N-GQDs/NiO is better than NiO nanoparticles. It can be attributed to the excellent optical properties of S,N-GQDs/NiO. It is well known that reactive oxygen species (ROS) is one of the major responsible for antibacterial mechanism. The optical properties of S,N-GQDs/NiO facilities ROS mechanism. The antibacterial activity of nanomaterials against a range of microorganisms varied considerably. The zone of inhibition was measured *Pseudomonas aeruginosa* (10 mm), *Escherichia coli* (16 mm), *Staphylococcus aureus* (19 mm), *and MRSA* (14 mm) for the S,N-GQDs/NiO nanocomposites (Table 2). The results in Table

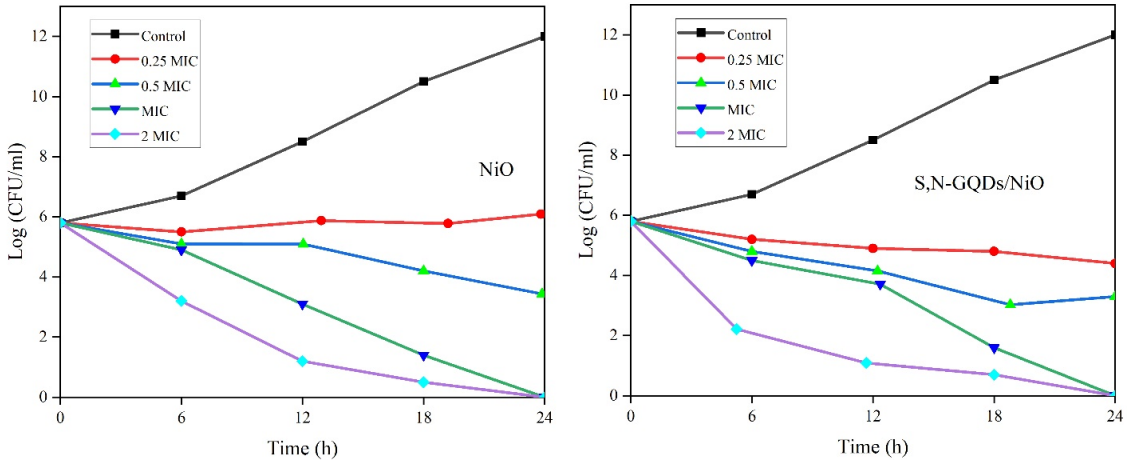

Fig. 5. Time-kill curve for *MRSA* strain by NiO nanoparticles and S,N-GQDs/NiO nanocomposites

2 confirms better antibacterial activity of S,N-GQDs/NiO nanocomposites in comparison with NiO nanoparticles. Time-kill Curve was applied for in-depth investigation of antibacterial activity at different times. Fig. 5 presents the time-kill Curve of NiO nanoparticles and S,N-GQDs/NiO nanocomposites against *MRSA*. First, it is obvious that antibacterial activity was increased with increasing the concentration of nanomaterials. Second, the antibacterial activity of S,N-GQDs/NiO nanocomposites is higher than NiO nanoparticles within 24 hours.

CONCLUSION

In conclusion, NiO nanoparticles and S,N-GQDs/NiO nanocomposites were prepared via a simple hydrothermal method. The structural and morphological properties of samples were analyzed via XRD, FTIE, UV-Vis, and FESEM analysis. Results confirmed the formation of NiO nanoparticles and S,N-GQDs/NiO nanocomposites with high purity. The optical properties of prepared S,N-GQDs/NiO nanocomposites lead to antibacterial application. So, the inhibition and bactericidal effects of NiO nanoparticles and S,N-GQDs/NiO nanocomposites were tested. Results revealed that *Staphylococcus aureus* showed the highest sensitivity since the lowest concentration of S,N-GQDs/NiO nanocomposites was applied via MIC and MBC value 0.4 and 0.8 mg/ml. The zone of inhibition was measured *Pseudomonas aeruginosa* (10 mm), *Escherichia coli* (16 mm), *Staphylococcus aureus* (19 mm), *and MRSA* (14 mm).

CONFLICT OF INTEREST

The authors declare that there is no conflict of interests regarding the publication of this manuscript.

REFERENCES

1. Zhang L, Huang C, Xu Y, Huang H, Zhao H, Wang J, et al. Synthesis and characterization of antibacterial polylactic acid film incorporated with cinnamaldehyde inclusions for fruit packaging. International Journal of Biological Macromolecules. 2020;164:4547-55.
2. Edgar KJ, Zhang H. Antibacterial modification of Lyocell fiber: A review. Carbohydrate Polymers. 2020;250:116932.
3. Dai J, Bai M, Li C, Cui H, Lin L. Advances in the mechanism of different antibacterial strategies based on ultrasound technique for controlling bacterial contamination in food industry. Trends in Food Science & Technology. 2020;105:211-22.
4. Fang T, Wang H, Cui Q, Rogers M, Dong P. Diversity of potential antibiotic-resistant bacterial pathogens and the effect of suspended particles on the spread of antibiotic resistance in urban recreational water. Water Research. 2018;145:541-51.
5. Jin M, Lu J, Chen Z, Nguyen SH, Mao L, Li J, et al. Antidepressant fluoxetine induces multiple antibiotics resistance in Escherichia coli via ROS-mediated mutagenesis. Environment International. 2018;120:421-30.
6. Hershberg R. Antibiotic-Independent Adaptive Effects of Antibiotic Resistance Mutations. Trends in Genetics. 2017;33(8):521-8.
7. Wu Z, Xu H, Xie W, Wang M, Wang C, Gao C, et al. Study on a novel antibacterial light-cured resin composite containing nano-MgO. Colloids and Surfaces B: Biointerfaces. 2020;188:110774.
8. Zhang Q, Zhang X, Cheng W, Li Z, Li Q. In situ-synthesis of calcium alginate nano-silver phosphate hybrid material with high flame retardant and antibacterial properties. International Journal of Biological Macromolecules. 2020;165:1615-25.
9. Ge X, Ren C, Ding Y, Chen G, Lu X, Wang K, et al. Micro/

nano-structured TiO_2 surface with dual-functional antibacterial effects for biomedical applications. Bioactive Materials. 2019;4:346-57.

10. Kalaycıoğlu Z, Kahya N, Adımcılar V, Kaygusuz H, Torlak E, Akın-Evingür G, et al. Antibacterial nano cerium oxide/chitosan/cellulose acetate composite films as potential wound dressing. European Polymer Journal. 2020;133:109777.
11. Guisbiers G, Mejía-Rosales S, Leonard Deepak F. Nanomaterial Properties: Size and Shape Dependencies. Journal of Nanomaterials. 2012;2012:1-2.
12. Jagiello K, Chomicz B, Avramopoulos A, Gajewicz A, Mikolajczyk A, Bonifassi P, et al. Size-dependent electronic properties of nanomaterials: How this novel class of nanodescriptors supposed to be calculated? Structural Chemistry. 2016;28(3):635-43.
13. Wang C, Levin AA, Karel J, Fabbrici S, Qian J, ViolBarbosa CE, et al. Size-dependent structural and magnetic properties of chemically synthesized Co-Ni-Ga nanoparticles. Nano Research. 2017;10(10):3421-33.
14. Chavali MS, Nikolova MP. Metal oxide nanoparticles and their applications in nanotechnology. SN Applied Sciences. 2019;1(6).
15. Prasanna SRVS, Balaji K, Pandey S, Rana S. Metal Oxide Based Nanomaterials and Their Polymer Nanocomposites. Nanomaterials and Polymer Nanocomposites: Elsevier; 2019. p. 123-44.
16. Zhu L, Awais M, Javed HMA, Mustafa MS, Tlili I, Khan SU, et al. Photo-catalytic pretreatment of biomass for anaerobic digestion using visible light and Nickle oxide (NiO_x) nanoparticles prepared by sol gel method. Renewable Energy. 2020;154:128-35.
17. Reddy KC, Sahatiya P, Santos-Sauceda I, Cortazar O, Ramirez-Bon R. One-step fabrication of 1D p-NiO nanowire/n-Si heterojunction: Development of self-powered ultraviolet photodetector. Applied Surface Science. 2020;513:145804.
18. Shanmuganandam K, Thanikaikarasan S, Venkata Ramanan M, Anichai J, Sebastian PJ. Enhancement of hydrogen energy from Casuarina equisetifolia using NiO–Pr_2O_3/TiO_2 and NiO/TiO_2 nano composites. International Journal of Hydrogen Energy. 2020;45(7):4152-60.
19. Kannan K, Radhika D, Nikolova MP, Sadasivuni KK, Mahdizadeh H, Verma U. Structural studies of bio-mediated NiO nanoparticles for photocatalytic and antibacterial activities. Inorganic Chemistry Communications. 2020;113:107755.
20. Khashan KS, Sulaiman GM, Abdul Ameer FA, Napolitano G. Synthesis, characterization and antibacterial activity of colloidal NiO nanoparticles. Pakistan journal of pharmaceutical sciences. 2016;29(2).
21. Pierrat P, Gaumet J-J. Graphene quantum dots: Emerging organic materials with remarkable and tunable luminescence features. Tetrahedron Letters. 2020;61(49):152554.
22. Younis MR, He G, Lin J, Huang P. Recent advances on graphene quantum dots for bioimaging applications. Frontiers in Chemistry. 2020;8:424.
23. Karthik K, Dhanuskodi S, Gobinath C, Prabukumar S, Sivaramakrishnan S. Multifunctional properties of microwave assisted CdO–NiO–ZnO mixed metal oxide nanocomposite: enhanced photocatalytic and antibacterial activities. Journal of Materials Science: Materials in Electronics. 2018 Apr;29(7):5459-71.
24. Sree GS, Botsa SM, Reddy BJM, Ranjitha KVB. Enhanced UV–Visible triggered photocatalytic degradation of Brilliant green by reduced graphene oxide based NiO and CuO ternary nanocomposite and their antimicrobial activity. Arabian Journal of Chemistry. 2020;13(4):5137-50.
25. Qu D, Zheng M, Du P, Zhou Y, Zhang L, Li D, et al. Highly luminescent S, N co-doped graphene quantum dots with broad visible absorption bands for visible light photocatalysts. Nanoscale. 2013;5(24):12272.
26. Hashemzadeh N, Hasanzadeh M, Shadjou N, Eivazi-Ziaei J, Khoubnasabjafari M, Jouyban A. Graphene quantum dot modified glassy carbon electrode for the determination of doxorubicin hydrochloride in human plasma. Journal of Pharmaceutical Analysis. 2016;6(4):235-41.